



HAL
open science

Mutations in GANAB, Encoding the Glucosidase II α Subunit, Cause Autosomal-Dominant Polycystic Kidney and Liver Disease.

Binu Porath, Vladimir G Gainullin, Emilie Cornec-Le Gall, Elizabeth K Dillinger, Christina M Heyer, Katharina Hopp, Marie E Edwards, Charles D Madsen, Sarah R Mauritz, Carly J Banks, et al.

► To cite this version:

Binu Porath, Vladimir G Gainullin, Emilie Cornec-Le Gall, Elizabeth K Dillinger, Christina M Heyer, et al.. Mutations in GANAB, Encoding the Glucosidase II α Subunit, Cause Autosomal-Dominant Polycystic Kidney and Liver Disease.. American Journal of Human Genetics, 2016, 98 (6), pp.1193-1207. 10.1016/j.ajhg.2016.05.004 . hal-01328055

HAL Id: hal-01328055

<https://hal.science/hal-01328055>

Submitted on 6 Feb 2017

HAL is a multi-disciplinary open access archive for the deposit and dissemination of scientific research documents, whether they are published or not. The documents may come from teaching and research institutions in France or abroad, or from public or private research centers.

L'archive ouverte pluridisciplinaire **HAL**, est destinée au dépôt et à la diffusion de documents scientifiques de niveau recherche, publiés ou non, émanant des établissements d'enseignement et de recherche français ou étrangers, des laboratoires publics ou privés.

**Mutations to *GANAB*, encoding the glucosidase IIa
subunit, cause autosomal dominant polycystic kidney
and liver disease**

Binu Porath^{1,#}, Vladimir G Gainullin^{1,#}, Emilie Cornec-Le Gall¹⁻³, Elizabeth K Dillinger⁴, Christina M Heyer¹, Katharina Hopp^{1,5}, Marie E Edwards¹, Charles D Madsen¹, Sarah R Mauritz¹, Carly J Banks¹, Saurabh Baheti⁶, Bharathi Reddy⁷, Jose Ignacio Herrero⁸⁻¹⁰, Jesus M Banales¹¹, Marie C Hogan¹, Velibor Tasic¹², Terry J Watnick¹³, Arlene B Chapman⁷, Cécile Vigneau¹⁴, Frédéric Lavainne¹⁵, Marie-Pierre Audrézet², Claude Ferec², Yannick Le Meur³, Vicente E Torres¹, the Genkyst, HALT PKD and CRISP studies and Peter C Harris^{*1,4}

¹Division of Nephrology and Hypertension, ⁴Department of Biochemistry and Molecular Biology, and ⁶Division of Biostatistics and Informatics, Mayo Clinic, Rochester, MN, 55905, USA, ²Department of Molecular Genetics, INSERM 1078, Brest, Brittany, 29200, France ³Department of Nephrology, University Hospital, Brest, Brittany, 29200, France. ⁵Division of Renal Diseases and Hypertension, University of Colorado Denver, Aurora, CO, 80202, USA, ⁷Section of Nephrology, University of Chicago, Chicago, IL, 60637, USA, ⁸Liver Unit, Clinica Universidad de Navarra, Pamplona, Navarra, 31009, Spain, ⁹Centro de Investigacion Biomedica en Red de Enfermedades Hepaticas y Digestivas (CIBERehd), Madrid, 28029, Spain. ¹⁰Instituto de Investigacion Sanitaria de Navarra (IdiSNA), Navarre, 31008, Spain, ¹¹Department of Liver and Gastrointestinal Diseases, Biodonostia Health Research Institute, Donostia University Hospital, UPV/EHU, CIBERehd, Ikerbasque, San Sebastian, 20014, Spain, ¹²Department of Pediatric Nephrology, University Children's Hospital, Skopje, 1010, Macedonia, ¹³Division of Nephrology, University of Maryland School of Medicine, Baltimore, MD, 21201, USA, ¹⁴Department of Nephrology, University Hospital, Rennes, Bretagne, 35000, France, ¹⁵Department of Nephrology, University Hospital, Nantes, Pays De La Loire, 44000, France.

#These authors contributed equally to the study

*Correspondence should be addressed to P.C.H. (harris.peter@mayo.edu)

ABSTRACT

Autosomal dominant polycystic kidney disease (ADPKD) is a common, progressive, adult onset disease that is an important cause of end stage renal disease (ESRD), requiring transplantation or dialysis. Mutations to *PKD1* or *PKD2* (~85% and ~15% of resolved cases, respectively) are the known causes of ADPKD. Extrarenal manifestations include an increased level of intracranial aneurysms (ICA) and polycystic liver disease (PLD), which can be severe and associated with significant morbidity. Autosomal dominant PLD (ADPLD) with no/very few renal cysts is a separate disorder caused by *PRKCSH*, *SEC63* or *LRP5* mutations. After screening, 7-10% of ADPKD and ~50% of ADPLD families were genetically unresolved (GUR), suggesting further genetic heterogeneity of both disorders. Whole exome sequencing of six GUR ADPKD families identified one with a missense mutation to *GANAB*, encoding the glucosidase II, α subunit (GII α). Since *PRKCSH* encodes the GII β subunit, *GANAB* was a strong ADPKD/ADPLD disease candidate. Sanger screening of 321 additional GUR families identified eight further likely mutations (six truncating), with a total of 20 affected individuals identified in seven ADPKD-like and two ADPLD-like families. The phenotype was mild PKD and variable, including severe, PLD. Analysis of *GANAB* null cells showed an absolute requirement of GII α for maturation and surface/ciliary localization of the ADPKD proteins (PC1 and PC2), with reduced mature PC1 seen in *GANAB*^{+/-} cells. PC1 surface localization in *GANAB*^{-/-} cells was rescued by wildtype but not mutant GII α . Overall we show that *GANAB* mutations cause ADPKD/ADPLD, with the cystogenesis likely driven by PC1 maturation defects.

INTRODUCTION

Autosomal dominant polycystic kidney disease (ADPKD) is one of the most common inherited disorders, ~1/1000 individuals affected worldwide, that is characterized by progressive kidney cyst development and expansion^{1; 2}. In ~50% of cases, ADPKD results in end stage kidney disease (ESRD), with 4-10% of ESRD worldwide due to ADPKD³. ADPKD is caused by mutations to *PKD1* [MIM: 601313] or *PKD2* [MIM: 173910] (~85% and ~15% of mutation resolved families, respectively)⁴⁻⁷. Genotype/phenotype studies indicate an average age at ESRD of 55.6y associated with truncating *PKD1* mutations, compared to 67.9y for *PKD1* non-truncating and 79.7y for *PKD2* [MIM: 613095]⁸. An earlier decline in renal function (measured by estimated glomerular filtration rate; eGFR) and larger kidneys (height adjusted, MRI determined total kidney volume; htTKV) are also associated with *PKD1* [MIM: 173900]^{6; 9}. The *PKD1* and *PKD2* proteins, polycystin-1 (PC1) and PC2, respectively, are membrane glycoproteins, with the primary cilium a likely functional site¹⁰. PC1 is cleaved at the GPS site and this cleavage is essential for function^{11; 12}. PC1 consists of two glycoforms of the N- and C-terminal GPS cleaved products – mature, Endoglycosidase H (EndoH) resistant (NTR/CTR) and immature, EndoH sensitive (NTS/CTS)¹³⁻¹⁵. The level of the mature glycoforms is associated with disease severity, and complexing with PC2 is critical for PC1 maturation and surface/ciliary localization^{13; 16; 17}.

In a number of comprehensive studies of the genes mutated in ADPKD, 7-10% of families are genetically unresolved (GUR)^{6-8; 18}. The typical finding of mild kidney disease in GUR cases⁶, suggests that few such families are explained by missed, fully penetrant mutations at the complex, segmentally duplicated, *PKD1* locus^{4; 19}. However, hypomorphic mutations at the existing loci, including due to mosaicism^{20; 21}, phenocopies associated with autosomal dominant tubulointerstitial kidney disease (ADTKD) loci^{22; 23} and phenotypic and screening mistakes likely

explain some unlinked/GUR families²⁴. Nevertheless, additional genetic heterogeneity seems possible.

Subjects affected by ADPKD have a ~5x higher risk of developing intracranial aneurysms (ICA)²⁵. However, polycystic liver disease (PLD) is the most frequent extra-renal complication in ADPKD, with a proportion of mainly females developing severe PLD, requiring surgical intervention^{26; 27}. Unlike PKD severity, severe PLD is not associated with a particular genic or *PKD1* allelic type²⁶. Isolated, autosomal dominant PLD (ADPLD [MIM: 174050]) is a separate inherited disorder where severe PLD can also occur, but renal cysts are absent/very rare²⁸. ADPLD is caused by mutations to *PRKCSH* [MIM: 177060], *SEC63* [MIM: 608648] or *LRP5*²⁹⁻³². *PRKCSH* encodes the glucosidase II, β subunit (GII β)^{33; 34}, with GII being an ER-resident enzyme that catalyzes hydrolysis of the middle and innermost glucose residues on peptide-bound oligosaccharide and triggers quality control assessment of glycoprotein folding through the calnexin/calreticulin cycle³⁵⁻⁴⁰. The SEC63 protein facilitates the translocation of secreted or membrane proteins across the endoplasmic reticulum (ER) membrane⁴¹⁻⁴⁴. Induced loss of *PrkcsH* or *Sec63* in mouse kidneys results in PKD, with an interactive network with PC1 and PC2 proposed, with PC1 as the rate-limiting component¹⁴. This suggests that *PRKCSH* mutation may act through PC1 depletion, although PC2 reduction has also been noted with *PrkcsH* depletion/loss^{45; 46}. There is strong evidence of further genetic heterogeneity in ADPLD, with only ~50% of affected individuals explained by the known genes mutated in this disease^{28; 47}.

In this study we have employed global and focused screening of GUR ADPKD/ADPLD families to identify a gene mutated in ADPKD/ADPLD. Characterization of cells null for this gene links the pathogenesis to the maturation and localization of PC1 and PC2.

SUBJECTS AND METHODS

Sample and data collection and clinical analysis

The relevant institutional review boards and ethics committees approved all studies, and participants gave informed consent. Blood samples for DNA isolation samples were collected from the proband and all available family members and isolated by standard methods in the Mayo Biospecimens Accessioning and Processing Core, or the Genkyst study. Clinical and imaging data was obtained by review of clinical records. TKV and TLV was measured from clinical MR and CT images at the Mayo Translational PKD Center employing the stereology method with the Analyze software or a semi-automated approach⁴⁸, and adjusted for height (htTKV or htTLV). Enlarged kidneys or livers were defined as the mean +2SD of normal htTKV or htTLV adjusted for average height^{27; 49}. Kidney function was calculated from clinical serum creatinine measurements using the CKD-EPI formula in adults⁵⁰ and the Schwarz formula in the pediatric case⁵¹ and expressed as ml/min/1.73m². Age at onset of high blood pressure was defined as when the affected individual started antihypertensive medication.

Whole exome sequencing (WES) and bioinformatics analysis

Families were defined GUR when no mutations were detected from Sanger sequencing and MLPA analysis of the *PKD1* and *PKD2* genes. In addition, the Genkyst cohort, including families PK20016 and PK20017, and P1174, were screened for *HNF1B* [MIM:189907] mutations, and families with a possible ADPLD diagnosis, including P1073, M472 and M656, were screened for *PRKCSH* and *SEC63* mutations.

Total genomic DNA was quantified using a Qubit 2.0 fluorometer (dsDNA BR assay kit) and quality checked with a NanoDrop. Subsequently, 250ng or 1µg of DNA was sheared by sonication (Covaris E210, 150-200bp), purified by AMPure XP beads (Agencourt), with shearing efficiency checked on a Agilent Bioanalyzer 2100 (DNA1000 assay). Whole exome capture and Illumina library preparation was performed using the Agilent SureSelectXT Human All Exon

V5+UTRs kit on an Agilent Bravo workstation. The enriched library was sequenced with 101bp paired-end reads on an Illumina HiSeq2000 in the Mayo Medical Genomics Facility. On average 3-4 exomes per lane were multiplexed. Genome_GPS v3.0.1 (Mayo Bioinformatics Core) was employed as a comprehensive secondary analysis pipeline for variant calling. In short, FASTQ files were aligned to the hg19 reference genome using Novoalign (VN:V2.08.01) with the following options: -hdrhd off -v 120 -c 4 -i PE 425,80 -x 5 -r Random, and realignment and recalibration performed using GATK (VN:3.3-0) best practices Version 3 for each family separately. Overall, 75.6% of mapped reads aligned to the captured region, and 98.9% of the captured region was covered at 10x read depth. Multi-sample variant calling was performed with the GATK (VN: 3.3-0) Haplotype Caller and variants filtered using the Variant Quality Score Recalibrator (VQSR) for both SNVs and InDels. Variant mining was performed employing Golden Helix SNP and Variation Suite v8 (SVS, Golden Helix, Inc). All families were analyzed independently with the following filtering procedure: (1) quality filter of read depth ($\geq 10X$) and genotype quality (≥ 20), (2) selection according to autosomal dominant sample genotype pattern, (3) removal of ExAC Browser variants with a minor allele frequency (MAF) of $>0.1\%$, and (4) characterization and removal of coding and non-coding SNVs within 14bp of the splice site and/or predicted to be neutral by one or more of six dbNSFP tools (tools selected as filter criteria were: SIFT, Polyphen2 HVAR, Mutation Taster, Mutation Assessor, FATHMM, and FATHMM MKL) and dbSCSNV (removed SNVs with Ada and RF scores <0.6). A list of variants that resulted after the SVS analysis is included in Table S1.

Sanger sequencing and mutation validation

Primers to amplify the 25 exons of *GANAB* (NM_198335.3), plus ~100bp of flanking IVS, were designed using MacVector 12.0.6 and 50ng of genomic DNA was used for PCR amplification (primers and PCR conditions available upon request). Sanger sequencing was performed at Beckman Coulter Genomics using standard approaches and variants identified with the

Mutation Surveyor software (Softgenetics) and designated on the 25 exon *GANAB* isoform and corresponding protein (NP_938149.2). Segregation analysis was performed where samples were available by sequencing the exonic fragment containing the mutation. Additionally, none of these variants were seen in the NHLBI Exome Sequence Project. Sanger sequencing detected amino acid changes were evaluated with the programs SIFT and Align GVGD and the atypical splicing change in M656 was evaluated with the BDGP Splice Site Prediction by Neural Network site. The origin of the *GANAB* families is: US, M263, M641, 290100, M656, M472; France, PK20016, PK20017; Macedonia, P1174; and Spain, P1073. One family came from the HALT PKD cohort, two from Genkyst, and the remainder from the Mayo PKD Center population.

Generation of targeted *GANAB* mutated cell lines using CRISPR/Cas9

Guide RNAs predicted to have the lowest off-targeting effect were cloned into pX330; SpCas9 and single guide RNA containing plasmid and verified by sequencing (see Table S2 for sequences). *GANAB* ex11-IVS12 was PCR amplified (primer sequences available on request) and the 550bp genomic product cloned into pCAG-EGxxFP⁵² using *Bam*HI and *Eco*RI restriction sites. Each gRNA was then co-transfected with p-CAG-EG-*GANAB*(11-IVS-12)-FP in RCTE cells and scored after 24hrs for EGFP positive cells. gRNA4 was selected as the most efficient cutter and used to generate cell lines. pX330-gRNA4 was transfected into WT RCTE cells by electroporation and the cells allowed to recover for 36hrs prior to splitting and re-seeding as single cell suspensions in a 96-well plate. Cells were grown for 10 days to establish single clone cell colonies, split two fold and re-seeded for screening. Screening was performed using genomic DNA extraction followed by amplification using *GANAB* ex11-IVS12 primers followed by the T7 mismatch assay. For this assay, PCR amplicons were denatured at 95°C for 2min and cooled gradually to 25°C at a rate of -2°C per second. The reaction mixture was then subjected to T7 endonuclease (T7E1, NEB) for 20min at 37°C and visualized in 2% agarose

gels. Clones were additionally screened using western blotting for GII α and Sanger sequencing.

Generating FLAG-GII α constructs with missense variants

C-terminal Myc-DDK tagged GII α (isoform 3, NM_198335.3) was obtained from Origene. Missense mutations were introduced by site-directed mutagenesis using Q5 high-fidelity polymerase (NEB) (primer sequences are shown in Table S3).

Western studies, glycosylation analysis and immunoprecipitation

For crude membrane protein purification, cells were grown to confluence, washed with Dulbecco's PBS (DPBS), scraped and reconstituted in LIS buffer (10mM Tris HCl pH 7.4, 2.5 mM MgCl₂, 1mM EDTA) plus protease inhibitors (Complete, Roche) and incubated on ice for 15min. Homogenized total membrane lysates were prepared by repeated passage through a 25.5 gauge needle and centrifugation at 4600 RPM for 5min. All procedures employed pre-chilled containers and were performed in the cold room to minimize protein loss to degradation. For IP, the crude membrane protein (75mg) pellet was solubilized in IP or high salt (500mM NaCl) IP buffer and samples pre-cleared with blank A/G agarose for 2hrs. Antibodies to PC1-CT and PC2 (YCE2) were added overnight and then incubated with 50ml of packed washed A/G Agarose (Thermo) for 2hrs. The agarose was washed 3x in IP buffer and once in ice-cold H₂O and the protein eluted in either LDS + TCEP or agarose was split into three equal parts (Untreated, EndoH and PNGaseF) and subjected to deglycosylation analyses. Purified membrane protein and IP eluates were deglycosylated with EndoH and PNGaseF according to the manufacturer's instructions (NEB). Twenty-five micrograms of input and 100% of the IP were loaded per SDS-PAGE lane.

Surface glycoprotein labeling and immunoprecipitation

Surface glycoprotein labeling of living cells was performed as previously described¹⁶. Monolayer cells in 10cm culture dishes were washed twice with ice-cold DPBS then oxidized at 4°C in 1mM

NaIO₄ containing DPBS (pH 7) for 30min, quenched with ice-cold 1mM glycerol in DPBS for 5min, and washed twice with ice-cold DPBS. Oxime ligation was performed in the presence of 10mM Aniline (Sigma) and 100µM Alkoxyamine-PEG₄-Biotin (Thermo) in 1% FBS supplemented ice-cold DPBS (pH 7.5) buffer for 1hr. Biotinylated cells were then washed 3x in PBS and scraped. Reaction specificity was ensured using Streptavidin-488 (Alexa Fluor) staining of a small sample of cells and visualized using fluorescent microscopy. Scraped cells were collected by centrifugation, subjected to crude membrane protein purification and solubilized in IP Buffer (20mM HEPES pH 7.5, 137mM NaCl, 1% NP-40, 10% (w/v) Glycerol, 2mM EDTA, 2.5 mM MgCl₂) supplemented with protease inhibitors (Roche) for 15mins. Non-solubilized protein was removed by centrifugation and discarded. Neutravidin agarose was washed in IP buffer 3x and 50ml of packed agarose added to solubilized membrane protein and agitated at 4°C for 2hrs. Samples were washed three times in IP buffer and once in ice-cold H₂O. Protein was eluted in either LDS + TCEP or agarose subjected to deglycosylation analyses. Tris-Acetate gels were washed with ultrapure water and stained using ProteoSilver stain kit according to manufacturer's instructions (Sigma) for silver staining.

Transfection, confocal microscopy, immunofluorescence (IF) and surface PC1 labeling

RCTE cells were split 1:2 the day before electroporation and transfected at ~80% confluency. Electroporation of RCTE cells was performed using the Biorad Gene Pulser with a square wave protocol: 110V, 25ms pulse and 0.2cm cuvettes (Biorad) in electroporation buffer (20mM HEPES, 135mM KCl, 2mM MgCl₂, 0.5% Ficoll 400, pH 7.6). TagGFP-PC2 and mCherry-PC1 used in this study were previously described¹⁶. RCTE cells were grown on glass cover slips, washed once with DPBS, fixed in 3.5% paraformaldehyde (PF) for 30min, permeabilized with 0.1% Triton in DPBS (pH 7.5), washed again in PBS, and incubated in blocking buffer (10% normal goat serum (NGS), 1% BSA, 0.1% Tween in PBS pH 7.5) for 30mins. After three PBS washes, primary antibodies were added in IF buffer (1% BSA, PBS pH 7.5, 0.1% Tween) for

2hrs at room temperature or overnight at 4°C with gentle agitation. After three PBS washes, conjugated secondary antibody (AlexaFluor, Invitrogen) was added for 1hr. DAPI was added for 1 min to stain nuclei.

For surface labeling of mCherry-PC1, transfected RCTE cells were cooled at 4°C for 15min, washed once in ice-cold PBS and pre-chilled mCherry antibody (BioVision), and incubated in 0.5% BSA in PBS for 30mins at 4°C. Cells were then fixed in 3.5% paraformaldehyde (PF) and conjugated secondary antibody added for 30mins in IF buffer. Confocal microscopy was performed using a Zeiss Axiovert equipped with Apotome.

For pH-shift/SDS IF, the fixation/antigen retrieval method was performed to visualize endogenous PC2 in MEFs. Cells were grown to 100% confluency and serum starved for 48hrs, fixed in 3% PF (pH 7.5) for 15min, fixed in 4% (PF pH 11 in 100mM borate buffer) for 15min, and then permeabilized in 5% SDS for 5min, to partially denature the protein. Subsequently, PC2 antibody (H280) staining performed overnight at a 1:200 dilution at 4°C, as described above.

Antibodies

PC1 NT IgG1 7e12⁵³ (WB 1/1000), PC1 CT Gt, EB08670, Everest Biotech (IP 1/250), PC2 Rb, H280, Santa Cruz (WB 1/5000, IF 1/200), PC2 IgG2a YCE2, Santa Cruz (WB 1/2000, IF 1/500), EGFR Rb, BD Transduction labs (WB 1/1000), Acetylated α -tubulin, IgG2b, Invitrogen (IF 1/5000), Anti-, mCherry Rb BioVision 5993-100 (Surface Labeling 1/1000), FLAG M2 IgG1 Sigma (IF 1/1000), α -Glucosidase II Abcam ab179805 (WB 1/2000).

RESULTS

Identification of *GANAB* as a gene mutated in ADPKD by whole exome sequencing

Following *PKD1* and *PKD2* mutation analysis for base pair and larger rearrangements, we identified 327 GUR families out of ~3600 screened. The origin of the GUR families was the HALT-PKD (64) ADPKD clinical trial, and the CRISP (16), and Genkyst (124) ADPKD observational studies. In addition, GUR families were included from screening ADPKD, and mild renal cystic disease families, including ones with PLD, at the Mayo PKD Center (123). While a firm clinical diagnosis of ADPKD was made in 247 GUR pedigrees, in 80 pedigrees the disease presentation was more atypical, with cystic kidney disease without kidney enlargement, although the vast majority exceeded the defined ultrasound or MRI criteria for ADPKD diagnosis^{54; 55}. In the 7 remaining families, the disease presentation was more consistent with ADPLD, although all but one had some renal cysts. *PRKCSH* and *SEC63* screening was also performed in these families before inclusion. Six multiplex ADPKD-like GUR families were screened by whole exome sequencing (WES) and standard screening methods employed to identify mutated, dominant genes (see Subjects and Methods), with detected genes/variants listed in Table S1. A missed *PKD1* mutation was identified in one family (M560).

From this WES analysis, one candidate gene, *GANAB*, encoding the catalytic α subunit of glucosidase II (GII α) appeared most promising since *PRKCSH* encodes the non-catalytic β subunit of this enzyme and mutations to this gene cause ADPLD. *GANAB* (Chr11q12.3) has two splice forms that *in silico* and RT-PCR analysis showed are approximately equally expressed in human kidney/liver (Figure S1): CDS: 2,988bp or 2,832bp; exons: 25 or 24 (inframe skipping of exon 6); genomic size: 21.9kb, AA: 966aa (~110kDa) or 944aa (~107kDa)^{37; 39}. We employed the larger splice form for mutation screening/designation and functional studies. ExAC exome data (60706 individuals) lists 5 loss of function (LoF) *GANAB* mutations compared to 49.7 expected (Probability of LoF intolerance [pLI]=1.0; see Subjects and Methods), a figure similar to *PKD2* (7/37.6; pLI=1.0), and consistent with it being a dominant cause of disease^{56; 57}.

The *GANAB* missense variant, c.1265G>T; p.Arg422Leu, was detected by WES in family M263 and found in the affected father and daughter but not the unaffected daughter (Figure 1A-C). *In silico* analysis, including conservation in a multi-sequence alignment (MSA) of orthologous proteins to yeast and related glucosidases showed and that this variant is highly predicted to be pathogenic (Figure 1D,E and legend). Both of the affected individuals had mild kidney and significant liver cystic disease (Figure 1F,G and Table 1).

Identification of further ADPKD families with *GANAB* mutations

Given that mutation to *GANAB* may explain unresolved ADPKD families, we analyzed our remaining GUR cohort of 321 families by Sanger sequencing of the coding region. From this analysis we identified eight additional families with *GANAB* mutations: three frameshifting, two splicing, one nonsense and two missense mutations (Table 1). Data from the Exome Aggregation Consortium (ExAC) showed that all the *GANAB* variants, except c.152_153delGA (reported once), have not been reported in the 60,706 unrelated individuals sequenced as part of various disease-specific and population genetic studies⁵⁶.

The *GANAB* frameshifting mutation, c.1914_1915delAG; p.Asp640Glnfs*77, was found in two families, M641 and 290100 (Figure 2A-E, Figures S2A,B, S3A, Table 1). In M641, two sisters had relatively mild PKD with variable liver cysts. The family history was unclear with the father dying at 75y with renal cell cancer but no reported cysts, with no information on the mother. Both sisters had ICA (see Figure 2 legend for details) and the father was reported to have a ruptured aneurysm. In family 290100, the father and son both had mild PKD, with multiple liver cysts in the father but not the son.

In family P1174, the *GANAB* missense variant, c.1214C>G; p.Thr405Arg, was found in three generations, including III-1 where renal cysts were detected incidentally in infancy (Figure 2F-H, Figures S2C, S3B, Table 1). The substituted residue is invariant in orthologs and conserved in

related proteins (Figure 2I,J). The *GANAB* splicing mutation, c.2690+2_+7del, was found in four affected family members in M656 (Figure 2K,L, Figures S2D, S3C,D, Table 1). All members had no to mild cystic liver disease and mild kidney disease, apart from II-3 who had multiple kidney cysts. Of note, the mother (without the *GANAB* mutation) had multiple cysts of unresolved etiology. PK20016 had the splicing mutation c.39-1G>C and PK20017 the nonsense mutation c.2176C>T; p.Arg726*, and both had only one known affected family member (Figure 3A-D, Figure S2E,F, Table 1). Both cases had multiple kidney cysts and a few liver cysts.

Identification of ADPLD-like families with *GANAB* mutations

In contrast to the described ADPKD cases, in families P1073 and M472 ADPLD was considered as a possible diagnosis, although a few renal cysts were present. P1073 had the missense mutation, c.2515C>T; p.Arg839Trp, which is at an invariant site in orthologs and segregates in three affected family members (Figure 3E-G, Figure S2G, Table 1). As indicated, there were very few renal cysts but multiple liver cysts, with the daughter, II-1, requiring a liver transplant at 43y. M472, II-1, with the *GANAB* frameshifting mutation c.152_153delGA; p.Arg51Lysfs*21 (Figure 3H,I, Figure S2H, Table 1), had a few small kidney cysts but severe PLD that required partial liver resections. A similar phenotype with less severe PLD was seen in II-2 (Figure S3E), although a sample was unavailable for mutation analysis.

Characterization of the effect of *GANAB* loss on PC1 and PC2 maturation/localization

From the genetic studies, mutation to *GANAB* was shown to be a cause of ADPKD/ADPLD, so we next explored the mechanism of pathogenesis by cellular analysis. CRISPR/Cas9 targeting of *GANAB* ex12 in human renal cortical tubular epithelial (RCTE) cells generated clones with biallelic frameshifting mutations (null; Clone C6) or a single in-frame deletion (heterozygous; E4; Figure S4A-D). Analysis of the PC complex immunocaptured with PC2 or PC1 CT antibodies in

GANAB^{-/-} cells showed that the PC1 N-terminal, mature product (PC1-NTR) was absent (Figure 4A,B). In contrast, full length (GPS uncleaved) PC1, PC1-NTS and PC2 were elevated, indicating that GII α plays a major role in PC1 maturation. We previously showed an interdependence of PC1 and PC2 for localization, including to cilia¹⁶, and so to assess localization of the polycystin complex PC2 was analyzed. Ciliary localization of PC2 was completely absent in *GANAB*^{-/-} cells, although cilia formed normally (Figure 4C, Figure S4E)¹⁶; ¹⁷. Since affected individuals harbored just one *GANAB* mutation we assayed *GANAB*^{+/-} cells and found a proportional, ~50%, depletion of PC1-NTR (Figure 4D,E). Analysis of the maturation of other membrane proteins (EGFR and E-cadherin) showed they were not, or only minorly, affected by loss of GII α (Figure 4A). Further analysis of terminally glycosylated proteins in *GANAB*^{-/-} cells did not suggest a global disruption of surface localized proteins (Figure S4F-H).

Functional analysis of *GANAB* mutations/variants

To determine the effect of *GANAB* loss on PC1 localization by immunofluorescence (IF) and to test the pathogenicity of detected *GANAB*/GII α variants, wildtype and *GANAB*^{-/-} cells were co-transfected with tagged PC1 and PC2 constructs (mCherry-PC1-V5 and GFP-PC2; Figure 5A,B)¹⁶. GII α loss prevented efficient surface localization of tagged PC1, which was restored by co-expression of WT FLAG-GII α (Figure 5A). Identified GII α missense mutations (p.Thr405Arg, p.Arg422Leu and p.Arg839Trp), expressed as FLAG-GII α constructs, failed to rescue PC1 surface localization in *GANAB*^{-/-} cells (Figure 5A), whereas three other variants considered likely neutral (c.284A>G; p.Gln95Arg, c.760A>G; p.Thr254Ala and c.991C>T; p.Arg331Cys) restored surface localization (Figure S5).

DISCUSSION

The combination of the human genetic studies and cellular analysis of *GANAB* null cells show that mutations to *GANAB* cause ADPKD/ADPLD, that loss/reduction of $GII\alpha$ • • associated with maturation and localization defects of PC1 and PC2, and that the identified mutations cannot rescue the PC1 localization defect.

The renal phenotype associated with *GANAB* mutation is consistently mild without renal insufficiency and any kidney enlargement due to a few large cysts. The *GANAB* phenotype is more similar to PKD2 than PKD1, but apparently even milder⁵⁸. In one case there was more severe PKD (M656; II-3), and here an undetermined cystogenic influence from the mother may be significant. Applying imaging diagnostic criteria developed in PKD1 and PKD2 families^{54; 55} may be unreliable in *GANAB* families even with a largely renal phenotype given the disease mildness and the variability within families. The significance of the vascular disease, noted in families M641, PK20017 and M472 is presently unclear. Only in M641 do the definitely affected sisters have ICA, with the vascular phenotypes in three other individuals in these families not proven to be *GANAB* mutation linked.

The liver disease is variable, ranging from no cysts to severe PLD requiring surgical intervention. The highly variable PLD phenotype is characteristic of ADPKD and ADPLD, with no data supporting allelic effects, although some evidence of familial clustering of severe PLD suggesting that genetic modifiers play a significant role^{26; 47}. It is interesting that *GANAB* mutation was identified as the cause of the disease in two of the seven ADPLD-like pedigrees studied, suggesting that the mutation detection rate may be higher in ADPLD families. Although there may be ascertainment bias since ADPKD was the diagnosis in the vast majority of screened families, the overall phenotype appears to involve more renal disease than described in *PRKCSH*⁵⁹. The reason for this as they are subunits of the same protein is unclear, with further analysis of *GANAB* in ADPLD and *PRKCSH* in ADPKD populations, required. We consider that phenotypes consistent with mild ADPKD as well as ADPLD with a few renal cysts

can be caused by *GANAB* mutation. Rather than considering ADPKD and ADPLD as strictly separate diseases, we suggest recording the full range of phenotypes associated with each gene where mutations are associated with ADPKD and/or ADPLD.

GANAB mutation accounts for ~3% of GUR ADPKD families (~0.3% total ADPKD), although since many GUR cases are likely missed *PKD1/PKD2* mutations (see Introduction and²⁴), it is probably responsible for a much greater proportion of missing genetic causes of ADPKD. In addition, due to the mild phenotype it is likely underdiagnosed, and in particular, may be more common in families with mild PKD and significant PLD.

Defects in glycosylation and protein trafficking underlie a large number of human diseases^{60; 61}, but the interesting aspect here is the specificity of the phenotype associated with disruption of a step in a process important for many proteins. GII functions in the early cargo recruitment steps of the calnexin/calreticulin cycle, which facilitates the quality control and maturation of transmembrane glycoproteins³⁵. *GANAB*^{-/-} cells and *S. pombe* mutants are viable without growth defects^{62; 63}, and we demonstrate a lack of global, surface glycoprotein deficiencies in *GANAB*^{-/-} cells, which suggests that endomannosidase activity and other chaperones and folding-assisting proteins can generally compensate for this loss, at least in non-stress conditions. The complexity due to protein size and extensive N-linked glycosylation may underlie the critical dependence of PC1 on GII and the calnexin/calreticulin cycle to achieve native folding. At this stage it is unclear if the enrichment of PLD associated with GII deficiency indicates that the liver is particularly vulnerable to reduction of this enzyme. The defect we observed in *GANAB*^{-/-} cells is complete disruption of PC1 maturation, increasing ER accumulation of cleaved PC1 with only a marginal effect on GPS-cleavage, in contrast to that described for SEC63 deficiency^{16; 62; 64; 65}. In RCTE cells, *GANAB* heterozygosity was associated with a ~50% reduction of PC1-NTR, a level predisposing to cyst development in association with stochastic, injury and/or somatic events^{13; 16; 66; 67}. However, further study is

required to fully understand quantitatively how PC1 maturation is influenced by GII dosage, studies that may lead to novel insights into a therapeutic role for cellular and molecular chaperones in ADPKD.

SUPPLEMENTAL DATA

Supplemental data includes one table and five figures.

ACKNOWLEDGEMENTS

Families and coordinators are thanked for their participation and efforts. The Exome Aggregation Consortium and groups that provided exome variant data, and Tatyana Masyuk for help with Family P1073, are also thanked. Other HALT PKD and CRISP investigators, including Drs. Grantham, Yu and Winklehofer (Kansas), Bae, Abebe, and Landsittel (Pittsburgh), Schrier and Brosnahan (Colorado), Perrone and Miskulin (Tufts), Braun (Cleveland Clinic), Steinman (Beth Israel), Mrug (UAB), Rahbari-Oskoui (Emory), Bennett (Portland), Flessner (NIDDK), Moore (Charlotte), Czarnecki (Brigham and Women's Hospital) are also thanked. NIDDK grant DK058816, the Mayo PKD Translational Center (DK090728), an American Heart Association Post-doctoral fellowship (BP), the Mayo Clinic Nephrology Training grant (T32DK007013, VGG), an American Society of Nephrology (ASN) Foundation Kidney Research Fellowship (ECLG) and ASN Ben J Lipps Fellowship (KH), Mayo Graduate School (EKD), the Zell Family Foundation, and Robert M. and Billie Kelley Pirnie supported the study. The CRISP and HALT PKD studies were supported by NIDDK cooperative agreements (DK056943, DK056956, DK056957, DK056961 and DK062410, DK062408, DK062402, DK082230, DK062411, DK062401, respectively) and National Center for Research Resources General Clinical Research Centers (RR000039, RR000585, RR000054, RR000051, RR023940, RR001032) and National Center for Advancing Translational Sciences Clinical and Translational Science Awards (RR025008, TR000454, RR024150, TR00135, RR025752, TR001064, RR025780, TR001082, RR025758, TR001102, RR033179, TR000001). The Genkyst cohort was supported by National Plans for Clinical Research (PHRC inter-regional 2010 for the Genkyst study and PHRC inter-regional 2013 for the GeneQuest study), Groupement Inter-Régional de Recherche Clinique et d'Innovation (GIRGI grand-ouest) and the French Society of Nephrology.

CONFLICT OF INTEREST STATEMENT

No authors declare a conflict of interest in this study.

WEB RESOURCES

URLs for websites employed in this study

ADPKD Mutation Database (<http://pkdb.mayo.edu>)

Align GVGD (<http://agvqd.iarc.fr>)

BDGP Splice Site Prediction by Neural Network (http://www.fruitfly.org/seq_tools/splice.html)

ExAC Browser (<http://exac.broadinstitute.org>)

GeneTests-GeneClinics (<https://www.genetests.org>)

National Center for Biotechnology Information (NCBI): Nucleotide

(<http://www.ncbi.nlm.nih.gov/nucleotide>)

NHLBI Exome Sequencing Project (<http://evs.gs.washington.edu/EVS/>)

Online Mendelian Inheritance in Man (<http://www.omim.org>)

SIFT (<http://sift.jcvi.org>)

REFERENCES

1. Torres, V.E., Harris, P.C., and Pirson, Y. (2007). Autosomal dominant polycystic kidney disease. *Lancet* 369, 1287-1301.
2. Harris, P.C., and Torres, V.E. (2009). Polycystic Kidney Disease. *Annu Rev Med* 60, 321-337.
3. Harris, P.C., and Torres, V.E. (2015). Polycystic Kidney Disease, Autosomal Dominant. In, R.A. Pagon, M.P. Adam, T.D. Bird, and et al., eds. (GeneReviews [Internet]; Genetic Disease Online Reviews at GeneTests-GeneClinics (University of Washington, Seattle) <http://www.genetests.org/>
4. Consortium, E.P.K.D. (1994). The polycystic kidney disease 1 gene encodes a 14 kb transcript and lies within a duplicated region on chromosome 16. *Cell* 77, 881-894.
5. Mochizuki, T., Wu, G., Hayashi, T., Xenophontos, S.L., Veldhusien, B., Saris, J.J., Reynolds, D.M., Cai, Y., Gabow, P.A., Pierides, A., et al. (1996). PKD2, a gene for polycystic kidney disease that encodes an integral membrane protein. *Science* 272, 1339-1342.
6. Heyer, C.M., Sundsbak, J.L., Abebe, K.Z., Chapman, A.B., Torres, V.E., Grantham, J.J., Bae, K.T., Schrier, R.W., Perrone, R., Braun, W.E., et al. (2016). Predicted mutation strength of nontruncating PKD1 mutations aids genotype-phenotype correlations in autosomal dominant polycystic kidney disease. *J Am Soc Nephrol* Jan 28 [Epub ahead of print].
7. Audrezet, M.P., Cornec-Le Gall, E., Chen, J.M., Redon, S., Quere, I., Creff, J., Benech, C., Maestri, S., Le Meur, Y., and Ferec, C. (2012). Autosomal dominant polycystic kidney disease: Comprehensive mutation analysis of PKD1 and PKD2 in 700 unrelated patients. *Hum Mutat* 33, 1239-1250.
8. Cornec-Le Gall, E., Audrezet, M.P., Chen, J.M., Hourmant, M., Morin, M.P., Perrichot, R., Charasse, C., Whebe, B., Renaudineau, E., Jousset, P., et al. (2013). Type of PKD1 Mutation Influences Renal Outcome in ADPKD. *J. Am. Soc. Nephrol.* 24, 1006-1013.
9. Grantham, J.J., Torres, V.E., Chapman, A.B., Guay-Woodford, L.M., Bae, K.T., King, B.F., Jr., Wetzel, L.H., Baumgarten, D.A., Kenney, P.J., Harris, P.C., et al. (2006). Volume progression in polycystic kidney disease. *N Engl J Med* 354, 2122-2130.
10. Ong, A.C., and Harris, P.C. (2015). A polycystin-centric view of cyst formation and disease: the polycystins revisited. *Kidney Int* 88, 699-710.
11. Qian, F., Boletta, A., Bhunia, A.K., Xu, H., Liu, L., Ahrabi, A.K., Watnick, T.J., Zhou, F., and Germino, G.G. (2002). Cleavage of polycystin-1 requires the receptor for egg jelly domain and is disrupted by human autosomal-dominant polycystic kidney disease 1- associated mutations. *Proc Natl Acad Sci U S A* 99, 16981-16986.
12. Wei, W., Hackmann, K., Xu, H., Germino, G., and Qian, F. (2007). Characterization of cis-autoproteolysis of polycystin-1, the product of human polycystic kidney disease 1 gene. *J. Biol. Chem.* 282, 21729-21737.
13. Hopp, K., Ward, C.J., Hommerding, C.J., Nasr, S.H., Tuan, H.F., Gainullin, V.G., Rossetti, S., Torres, V.E., and Harris, P.C. (2012). Functional polycystin-1 dosage governs autosomal dominant polycystic kidney disease severity. *J. Clin. Invest.* 122, 4257-4273.
14. Fedeles, S.V., Tian, X., Gallagher, A.R., Mitobe, M., Nishio, S., Lee, S.H., Cai, Y., Geng, L., Crews, C.M., and Somlo, S. (2011). A genetic interaction network of five genes for human polycystic kidney and liver diseases defines polycystin-1 as the central determinant of cyst formation. *Nat Genet* 43, 639-647.
15. Kurbegovic, A., Kim, H., Xu, H., Yu, S., Cruanes, J., Maser, R.L., Boletta, A., Trudel, M., and Qian, F. (2014). Novel functional complexity of polycystin-1 by GPS cleavage in vivo: role in polycystic kidney disease. *Mol Cell Biol* 34, 3341-3353.
16. Gainullin, V.G., Hopp, K., Ward, C.J., Hommerding, C.J., and Harris, P.C. (2015). Polycystin-1 maturation requires polycystin-2 in a dose-dependent manner. *J Clin Invest* 125, 607-620.

17. Kim, H., Xu, H., Yao, Q., Li, W., Huang, Q., Outeda, P., Cebotaru, V., Chiaravalli, M., Boletta, A., Piontek, K., et al. (2014). Ciliary membrane proteins traffic through the Golgi via a Rabep1/GGA1/Arl3-dependent mechanism. *Nat Commun* 5, 5482.
18. Rossetti, S., Consugar, M.B., Chapman, A.B., Torres, V.E., Guay-Woodford, L.M., Grantham, J.J., Bennett, W.M., Meyers, C.M., Walker, D.L., Bae, K., et al. (2007). Comprehensive molecular diagnostics in autosomal dominant polycystic kidney disease. *J Am Soc Nephrol* 18, 2143-2160.
19. Loftus, B.J., Kim, U.-J., Sneddon, V.P., Kalush, F., Brandon, R., Fuhrmann, J., Mason, T., Crosby, M.L., Barnstead, M., Cronin, L., et al. (1999). Genome duplications and other features in 12 Mbp of DNA sequence from human chromosome 16p and 16q. *Genomics* 60, 295-308.
20. Consugar, M.B., Wong, W.C., Lundquist, P.A., Rossetti, S., Kubly, V., Walker, D.L., Rangel, L.J., Aspinwall, R., Niaduet, W.P., Ozen, S., et al. (2008). Characterization of large rearrangements in autosomal dominant polycystic kidney disease and the *PKD1/TSC2* contiguous gene syndrome. *Kidney Int* 74, 1468-1479.
21. Tan, A.Y., Blumenfeld, J., Michaeel, A., Donahue, S., Bobb, W., Parker, T., Levine, D., and Rennert, H. (2015). Autosomal dominant polycystic kidney disease caused by somatic and germline mosaicism. *Clin Genet* 87, 373-377.
22. Heidet, L., Decramer, S., Pawtowski, A., Moriniere, V., Bandin, F., Knebelmann, B., Lebre, A.S., Faguer, S., Guignon, V., Antignac, C., et al. (2010). Spectrum of *HNF1B* mutations in a large cohort of patients who harbor renal diseases. *Clin J Am Soc Nephrol* 5, 1079-1090.
23. Eckardt, K.U., Alper, S.L., Antignac, C., Bleyer, A.J., Chauveau, D., Dahan, K., Deltas, C., Hosking, A., Knoch, S., Rampoldi, L., et al. (2015). Autosomal dominant tubulointerstitial kidney disease: diagnosis, classification, and management--A KDIGO consensus report. *Kidney Int* 88, 676-683.
24. Paul, B.M., Consugar, M.B., Ryan Lee, M., Sundsbak, J.L., Heyer, C.M., Rossetti, S., Kubly, V.J., Hopp, K., Torres, V.E., Coto, E., et al. (2014). Evidence of a third ADPKD locus is not supported by re-analysis of designated PKD3 families. *Kidney Int* 85, 383-392.
25. Pirson, Y., Chauveau, D., and Torres, V. (2002). Management of cerebral aneurysms in autosomal dominant polycystic kidney disease. *J Am Soc Nephrol* 13, 269-276.
26. Chebib, F.T., Jung, Y., Heyer, C.M., Irazabal, M.V., Hogan, M.C., Harris, P.C., Torres, V.E., and El-Zoghby, Z.M. (2016). Effect of genotype on the severity and volume progression of polycystic liver disease in ADPKD. *Nephrol Dial Transplant* Feb 29 [Epub ahead of print].
27. Hogan, M.C., Abebe, K., Torres, V.E., Chapman, A.B., Bae, K.T., Tao, C., Sun, H., Perrone, R.D., Steinman, T.I., Braun, W., et al. (2015). Liver Involvement in Early Autosomal-Dominant Polycystic Kidney Disease. *Clin Gastroenterol Hepatol* 13, 155-164.
28. Hoevenaren, I.A., Wester, R., Schrier, R.W., McFann, K., Doctor, R.B., Drenth, J.P., and Everson, G.T. (2007). Polycystic liver: clinical characteristics of patients with isolated polycystic liver disease compared with patients with polycystic liver and autosomal dominant polycystic kidney disease. *Liver Int* 28, 264-270.
29. Drenth, J.P., Te Morsche, R.H., Smink, R., Bonifacino, J.S., and Jansen, J.B. (2003). Germline mutations in *PRKCSH* are associated with autosomal dominant polycystic liver disease. *Nat Genet* 33, 345-347.
30. Li, A., Davila, S., Furu, L., Qian, Q., Tian, X., Kamath, P.S., King, B.F., Torres, V.E., and Somlo, S. (2003). Mutations in *PRKCSH* Cause Isolated Autosomal Dominant Polycystic Liver Disease. *Am J Hum Genet* 72, 691-703.
31. Davila, S., Furu, L., Gharavi, A.G., Tian, X., Onoe, T., Qian, Q., Li, A., Cai, Y., Kamath, P.S., King, B.F., et al. (2004). Mutations in *SEC63* cause autosomal dominant polycystic liver disease. *Nat Genet* 36, 575-577.
32. Cnossen, W.R., Te Morsche, R.H., Hoischen, A., Gilissen, C., Chrispijn, M., Venselaar, H., Mehdi, S., Bergmann, C., Veltman, J.A., and Drenth, J.P. (2014). Whole-exome sequencing reveals LRP5

- mutations and canonical Wnt signaling associated with hepatic cystogenesis. *Proc Natl Acad Sci USA* *111*, 5343-5348.
33. Sakai, K., Hirai, M., Minoshima, S., Kudoh, J., Fukuyama, R., and Shimizu, N. (1989). Isolation of cDNAs encoding a substrate for protein kinase C: nucleotide sequence and chromosomal mapping of the gene for a human 80K protein. *Genomics* *5*, 309-315.
 34. Trombetta, E.S., Simons, J.F., and Helenius, A. (1996). Endoplasmic reticulum glucosidase II is composed of a catalytic subunit, conserved from yeast to mammals, and a tightly bound noncatalytic HDEL-containing subunit. *J Biol Chem* *271*, 27509-27516.
 35. Xu, C., and Ng, D.T. (2015). Glycosylation-directed quality control of protein folding. *Nat Rev Mol Cell Biol* *16*, 742-752.
 36. D'Alessio, C., and Dahms, N.M. (2015). Glucosidase II and MRH-domain containing proteins in the secretory pathway. *Curr Protein Pept Sci* *16*, 31-48.
 37. Trembl, K., Meimaroglou, D., Hentges, A., and Bause, E. (2000). The alpha- and beta-subunits are required for expression of catalytic activity in the hetero-dimeric glucosidase II complex from human liver. *Glycobiology* *10*, 493-502.
 38. Tannous, A., Pisoni, G.B., Hebert, D.N., and Molinari, M. (2015). N-linked sugar-regulated protein folding and quality control in the ER. *Semin Cell Dev Biol* *41*, 79-89.
 39. Pelletier, M.F., Marcil, A., Sevigny, G., Jakob, C.A., Tessier, D.C., Chevet, E., Menard, R., Bergeron, J.J., and Thomas, D.Y. (2000). The heterodimeric structure of glucosidase II is required for its activity, solubility, and localization in vivo. *Glycobiology* *10*, 815-827.
 40. Deprez, P., Gautschi, M., and Helenius, A. (2005). More than one glycan is needed for ER glucosidase II to allow entry of glycoproteins into the calnexin/calreticulin cycle. *Mol Cell* *19*, 183-195.
 41. Rothblatt, J.A., Deshaies, R.J., Sanders, S.L., Daum, G., and Schekman, R. (1989). Multiple genes are required for proper insertion of secretory proteins into the endoplasmic reticulum in yeast. *J Cell Biol* *109*, 2641-2652.
 42. Sadler, I., Chiang, A., Kurihara, T., Rothblatt, J., Way, J., and Silver, P. (1989). A yeast gene important for protein assembly into the endoplasmic reticulum and the nucleus has homology to DnaJ, an *Escherichia coli* heat shock protein. *J Cell Biol* *109*, 2665-2675.
 43. Deshaies, R.J., Sanders, S.L., Feldheim, D.A., and Schekman, R. (1991). Assembly of yeast Sec proteins involved in translocation into the endoplasmic reticulum into a membrane-bound multisubunit complex. *Nature* *349*, 806-808.
 44. Skowronek, M.H., Rotter, M., and Haas, I.G. (1999). Molecular characterization of a novel mammalian DnaJ-like Sec63p homolog. *Biol Chem* *380*, 1133-1138.
 45. Gao, H., Wang, Y., Wegierski, T., Skouloudaki, K., Putz, M., Fu, X., Engel, C., Boehlke, C., Peng, H., Kuehn, E.W., et al. (2010). PRKCSH/80K-H, the protein mutated in polycystic liver disease, protects polycystin-2/TRPP2 against HERP-mediated degradation. *Hum Mol Genet* *19*, 16-24.
 46. Hofherr, A., Wagner, C., Fedeles, S., Somlo, S., and Kottgen, M. (2014). N-glycosylation determines the abundance of the transient receptor potential channel TRPP2. *J Biol Chem* *289*, 14854-14867.
 47. Waanders, E., te Morsche, R.H., de Man, R.A., Jansen, J.B., and Drenth, J.P. (2006). Extensive mutational analysis of PRKCSH and SEC63 broadens the spectrum of polycystic liver disease. *Hum Mut* *27*, 830.
 48. Kline, T.L., Korfiatis, P., Edwards, M.E., Warner, J.D., Irazabal, M.V., King, B.F., Torres, V.E., and Erickson, B.J. (2016). Automatic total kidney volume measurement on follow-up magnetic resonance images to facilitate monitoring of autosomal dominant polycystic kidney disease progression. *Nephrol Dial Transplant* *31*, 241-248.
 49. Cheong, B., Muthupillai, R., Rubin, M.F., and Flamm, S.D. (2007). Normal values for renal length and volume as measured by magnetic resonance imaging. *Clin J Am Soc Nephrol* *2*, 38-45.

50. Levey, A.S., Stevens, L.A., Schmid, C.H., Zhang, Y.L., Castro, A.F., 3rd, Feldman, H.I., Kusek, J.W., Eggers, P., Van Lente, F., Greene, T., et al. (2009). A new equation to estimate glomerular filtration rate. *Ann. Intern. Med.* *150*, 604-612.
51. Schwartz, G.J., Haycock, G.B., Edelmann, C.M., Jr., and Spitzer, A. (1976). A simple estimate of glomerular filtration rate in children derived from body length and plasma creatinine. *Pediatrics* *58*, 259-263.
52. Mashiko, D., Fujihara, Y., Satouh, Y., Miyata, H., Isotani, A., and Ikawa, M. (2013). Generation of mutant mice by pronuclear injection of circular plasmid expressing Cas9 and single guided RNA. *Sci Rep* *3*, 3355.
53. Ong, A.C.M., Harris, P.C., Davies, D.R., Pritchard, L., Rossetti, S., Biddolph, S., Vaux, D.J.T., Migone, N., and Ward, C.J. (1999). Polycystin-1 expression in PKD1, early onset PKD1 and TSC2/PKD1 cystic tissue: implications for understanding cystogenesis. *Kidney Int* *56*, 1324-1333.
54. Pei, Y., Obaji, J., Dupuis, A., Paterson, A.D., Magistroni, R., Dicks, E., Parfrey, P., Cramer, B., Coto, E., Torra, R., et al. (2009). Unified criteria for ultrasonographic diagnosis of ADPKD. *J. Am. Soc. Nephrol.* *20*, 205-212.
55. Pei, Y., Hwang, Y.H., Conklin, J., Sundsbak, J.L., Heyer, C.M., Chan, W., Wang, K., He, N., Rattansingh, A., Atri, M., et al. (2015). Imaging-based diagnosis of autosomal dominant polycystic kidney disease. *J. Am. Soc. Nephrol.* *26*, 746-753.
56. (ExAC), E.A.C. (2016). Exome Aggregation Consortium (ExAC) Cambridge, MA (URL: <http://exac.broadinstitute.org>). In. (
57. Lek, M., Karczewski, K., Minikel, E., Samocha, K., Banks, E., Fennell, T., O'Donnell-Luria, A., Ware, J., Hill, A., Cummings, B., et al. (2015). Analysis of protein-coding genetic variation in 60,706 humans. *bioRxiv*.
58. Harris, P.C., Bae, K., Rossetti, S., Torres, V.E., Grantham, J.J., Chapman, A., Guay-Woodford, L., King, B.F., Wetzel, L.H., Baumgarten, D., et al. (2006). Cyst number but not the rate of cystic growth is associated with the mutated gene in ADPKD. *J Am Soc Nephrol* *17*, 3013-3019.
59. Cnossen, W.R., and Drenth, J.P. (2014). Polycystic liver disease: an overview of pathogenesis, clinical manifestations and management. *Orphanet J Rare Dis* *9*, 69.
60. Hung, M.C., and Link, W. (2011). Protein localization in disease and therapy. *J Cell Sci* *124*, 3381-3392.
61. Hennet, T., and Cabalzar, J. (2015). Congenital disorders of glycosylation: a concise chart of glycolyx dysfunction. *Trends Biochem Sci* *40*, 377-384.
62. D'Alessio, C., Fernandez, F., Trombetta, E.S., and Parodi, A.J. (1999). Genetic evidence for the heterodimeric structure of glucosidase II. The effect of disrupting the subunit-encoding genes on glycoprotein folding. *J Biol Chem* *274*, 25899-25905.
63. Reitman, M.L., Trowbridge, I.S., and Kornfeld, S. (1982). A lectin-resistant mouse lymphoma cell line is deficient in glucosidase II, a glycoprotein-processing enzyme. *J Biol Chem* *257*, 10357-10363.
64. Fedeles, S.V., So, J.S., Shrikhande, A., Lee, S.H., Gallagher, A.R., Barkauskas, C.E., Somlo, S., and Lee, A.H. (2015). Sec63 and Xbp1 regulate IRE1alpha activity and polycystic disease severity. *J Clin Invest* *125*, 1955-1967.
65. Moore, S.E., and Spiro, R.G. (1990). Demonstration that Golgi endo- α -D-mannosidase provides a glucosidase-independent pathway for the formation of complex N-linked oligosaccharides of glycoproteins. *J Biol Chem* *265*, 13104-13112.
66. Gallagher, A.R., Germino, G.G., and Somlo, S. (2010). Molecular advances in autosomal dominant polycystic kidney disease. *Adv Chronic Kidney Dis* *17*, 118-130.
67. Takakura, A., Contrino, L., Zhou, X., Bonventre, J.V., Sun, Y., Humphreys, B.D., and Zhou, J. (2009). Renal injury is a third hit promoting rapid development of adult polycystic kidney disease. *Hum. Mol. Genet.* *18*, 2523-2531.

68. Urribarri, A.D., Munoz-Garrido, P., Perugorria, M.J., Erice, O., Merino-Azpitarte, M., Arbelaz, A., Lozano, E., Hijona, E., Jimenez-Aguero, R., Fernandez-Barrena, M.G., et al. (2014). Inhibition of metalloprotease hyperactivity in cystic cholangiocytes halts the development of polycystic liver diseases. *Gut* 63, 1658-1667.

FIGURE LEGENDS

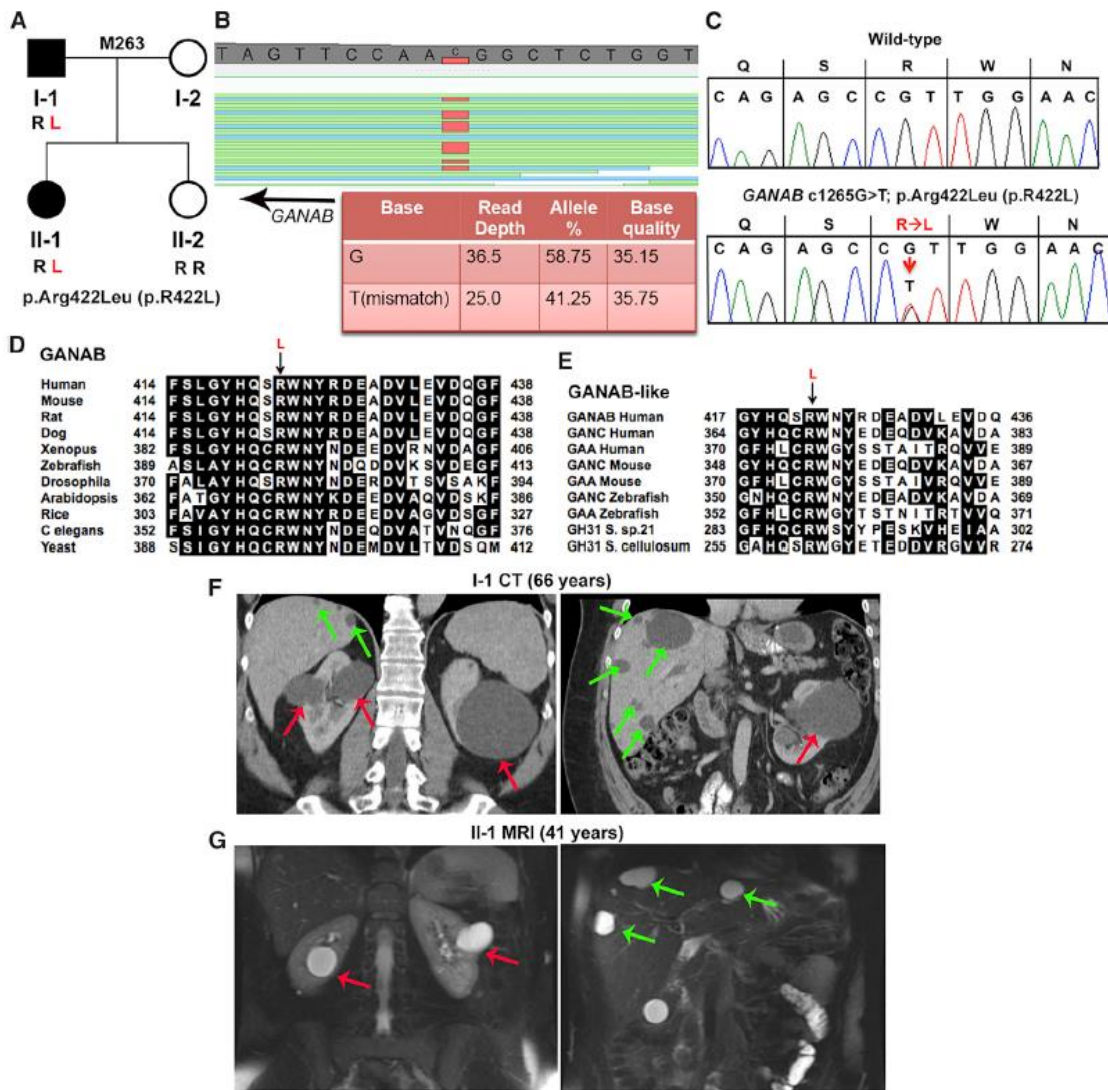


Figure 1: WES analysis reveals a *GANAB* variant c.1265G>T; p.R422L in family M263 as the likely mutation

(A) Pedigree M263 showing that the two affected individuals (I-1 and II-1; black shaded) segregated the *GANAB*, c.1265G>T; p.Arg422Leu (p.R422L; ex12) missense mutation, but the unaffected daughter, II-2 (no cysts detected on ultrasound, 30y), did not. (B) GenomeBrowse (SVS, Golden Helix Inc.) view of the WES results from II-1 showing the *GANAB* variant

c.1265G>T (reverse strand), with details of the reads tabulated below. **(C)** Sanger sequencing confirmation in II-1 of heterozygous *GANAB* variant c.1265G>T; p.Arg422Leu (p.R422L), compared to wild type. **(D)** MSA of GII α orthologous proteins showing invariance of Arg422 from human to yeast. *In silico* analysis of the likely pathogenicity of GII α p.Arg422Leu (p.R422L) showed variant scores (SIFT=0.00; Align GVGD=C65) characteristic of a highly likely pathogenic mutation. **(E)** MSA of related glucosidases, GANC (neutral alpha-glucosidase C) and GAA (lysosomal alpha-glucosidase) of various eukaryotic species and prokaryotic GH31 (glycosyl hydrolase family 31) showing invariant conservation of GII α Arg422. **(F)** CT scan with contrast of kidneys and liver of I-1 at 66y showing a few large kidney cysts (red arrows) and multiple scattered liver cysts (green arrows). **(G)** T2-weighted MR images from II-1 at 41y showing a few kidney (red arrows) and liver cysts (green arrows).

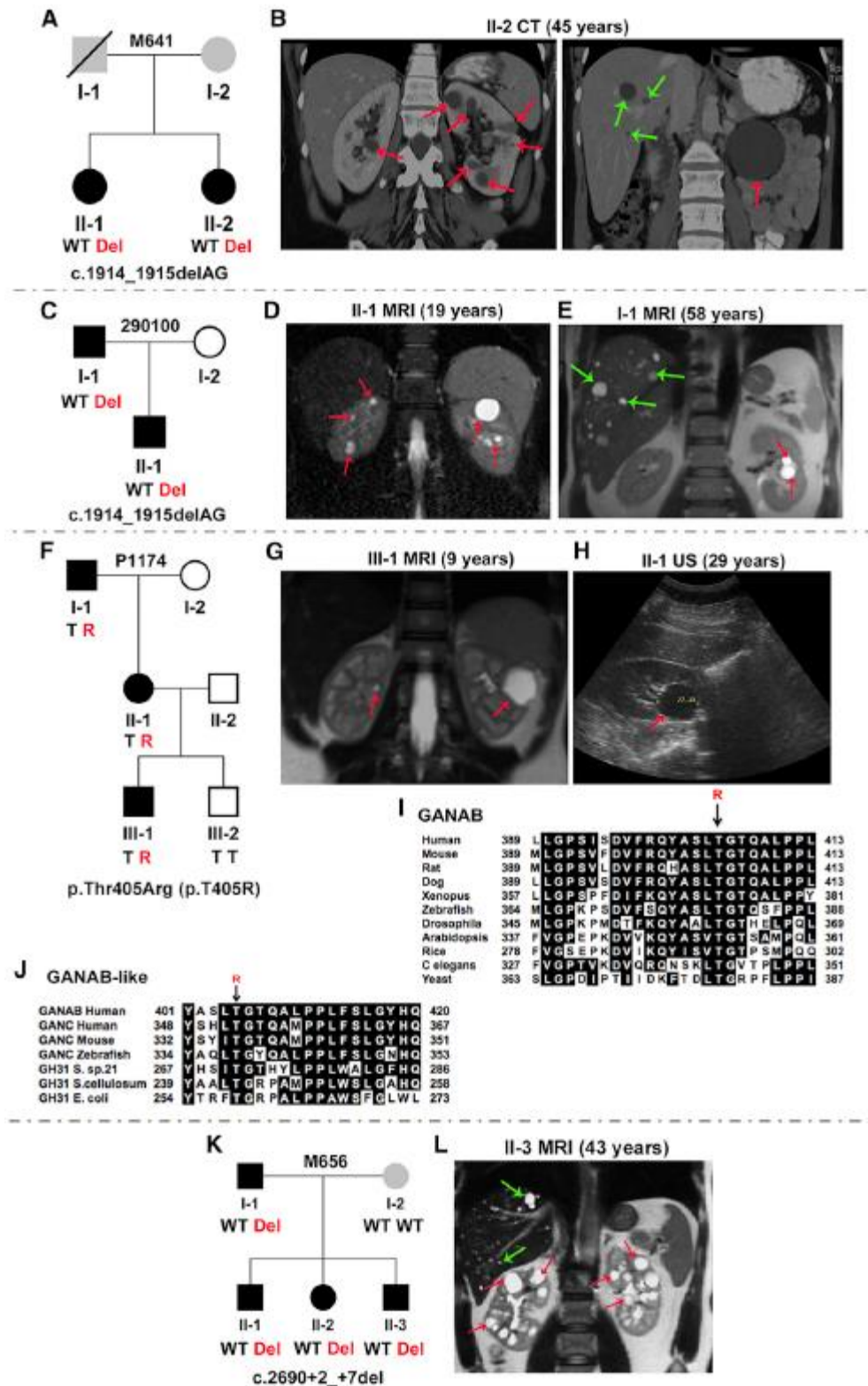


Figure 2: Characterization of *GANAB* mutations in four ADPKD families.

(A) Pedigree M641 with c.1914_1915delAG; p.Asp640Glnfs*77 (ex17) in two affected siblings.

Both sisters had basilar tip aneurysms and II-2 also had two aneurysms detected on the left

middle cerebral artery. The affected status of the parents is unclear (gray shading); I-1 had renal cell carcinoma and a ruptured aneurysm but no reported PKD. **(B)** CT scan of kidneys and liver from II-2 showing multiple kidney and occasional liver cysts. **(C)** Pedigree 290100 showing c.1914_1915delAG in the father and son. MR images of II-1 **(D)** showing a few kidney but no hepatic cysts and I-1 **(E)** with a few kidney and scattered liver cysts. **(F)** Pedigree P1174 has c.1214C>G; p.Thr405Arg (p.T405R; ex11), in three affected individuals; III-2, with no cysts detected by ultrasound (US) at 5y, did not have the variant. **(G)** MRI of III-1 showing bilateral kidney cysts and US image of II-1 **(H)** with a single large renal cyst. **(I)** MSA of *GANAB* (GII α) orthologs showing Thr405 invariant across species. *In silico* mutation analysis highly predicts p.Thr405Arg (p.T405R) as pathogenic (SIFT=0.00, Align GVGD=C65). **(J)** MSA of *GANAB*-like proteins shows invariant conservation of this residue. **(K)** Pedigree M656 segregates c.2690+2_+7del (IVS20) in four affected members. Splicing predictions showed complete loss of the donor site. The mother (I-2), without the *GANAB* mutation, has ~5 kidney and ~30 liver cysts but no detected *PKD1*, *PKD2*, *PRKCSH*, or *SEC63* mutation. **(L)** MR images of II-3 showing small hepatic and multiple renal cysts. Red and green arrows indicate kidney and liver cysts, respectively. Just representative cysts are highlighted where multiple cysts are present.

Figure 3: Characterization of *GANAB* variants in four families, including P1073 and M472 with an ADPLD diagnosis

(A) Pedigree PK20016 with the splicing mutation, c.39-1G>C (IVS1). The family history is unclear with samples unavailable, but one large renal cyst was reported in I-1. (B) CT-scan of II-1 showing bilateral kidney cysts and occasional hepatic cysts. (C) Pedigree PK20017 with c.2176C>T; p.Arg726* (p.R726*; ex18), in the proband II-1. Lack of DNA samples and clinical information precluded determining family history. II-2 died at 55y from a ruptured intracranial aneurysm, but his PKD status was unknown. (D) Ultrasound examination of II-1 shows several liver (left), and kidney cysts (right). (E) Pedigree P1073 segregates c.2515C>T; p.Arg839Trp (p.R839W; ex22), in three affected individuals. (F) CT scan of II-1 showing very few kidney cysts (left), but severe PLD (right). Gross images of the liver of this subject have been published⁶⁸. (G) MSA of *GANAB* (GII α) orthologs showing invariant conservation of Arg839 across species. *In silico* mutation analysis highly predicted p.Arg839Trp (p.R839W) as pathogenic (SIFT=0.00, Align GVGD=C65). (H) Pedigree M472 with c.152_153delGA; p.Arg51Lysfs*21 (p.R51fs; ex3) in II-1. (I) MR images from II-1 show a few renal cysts (left) but significant PLD, with this image subsequent to earlier resections (Table 1). No sample was available from II-2, but imaging showed also predominant PLD (Figure S3E). Parental DNA samples were unavailable and clinical information limited to determine family history, but I-1 was reported to have had a cerebral hemorrhage. Red and green arrows indicate kidney and liver cysts, respectively. Just representative cysts are highlighted where multiple cysts are presents.

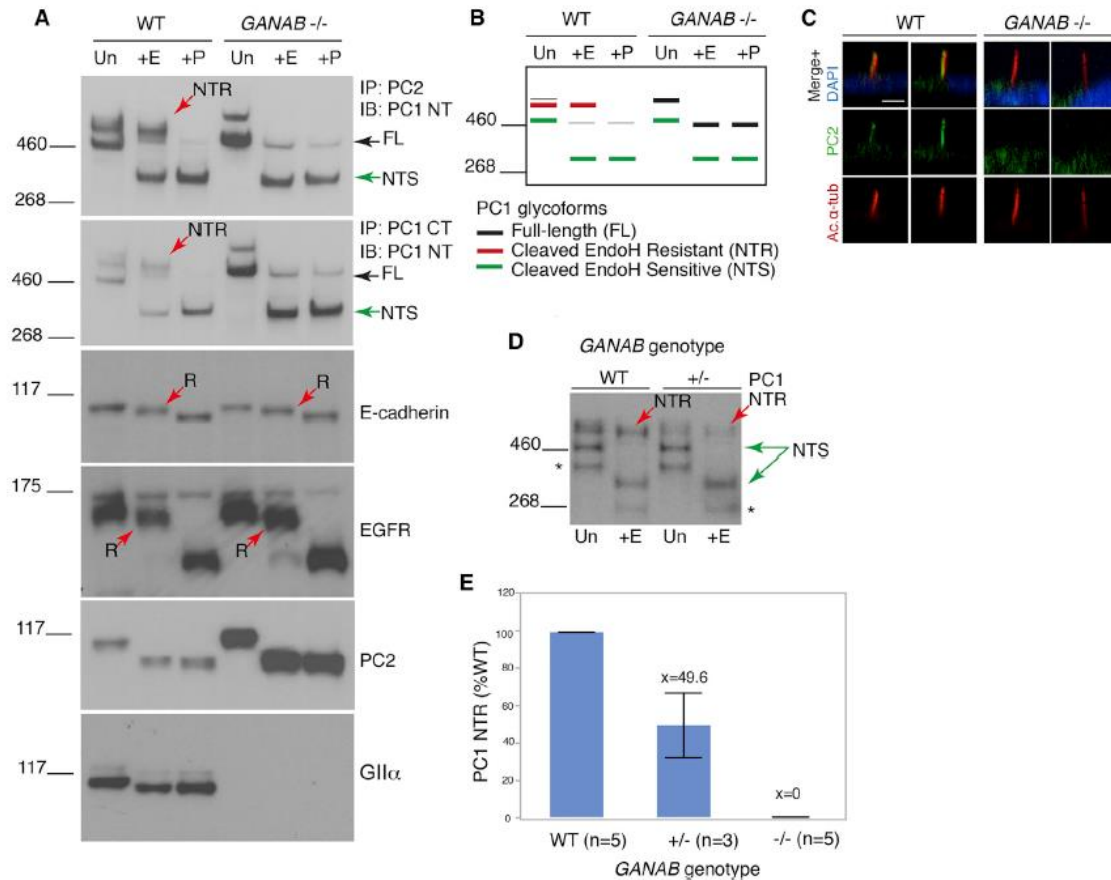


Figure 4. GII α is required for PC1 ER-exit and maturation

(A) Deglycosylation analysis of wildtype (WT) and *GANAB*^{-/-} RCTE membrane protein treated with EndoH (+E), PNGaseF (+P) or untreated (Un). IP was used to enrich the PC1 complex with C-terminal PC1 (CT) or PC2 (YCE2) antibodies and immunodetected with the N-terminal PC1 (NT) antibody (7e12). Complete loss of the mature PC1 glycoform¹⁶ (NTR; red arrow) was observed in *GANAB*^{-/-} cells, with full length PC1 (FL) and PC1-NTS becoming more abundant. Mature E-cadherin and epidermal growth factor receptor (EGFR) were not or only marginally affected by *GANAB* loss, with the EndoH resistant protein (R, red arrow) persisting. No PC2 EndoH resistant form was noted¹⁶, but the protein was upregulated in *GANAB*^{-/-} cells. Loss of WT GII α was confirmed in *GANAB*^{-/-} cells using a C-terminal antibody. **(B)** Schematic representation of the observed PC1 banding pattern in WT and *GANAB*^{-/-} cells **(A)**. **(C)** Confocal Z-stack rendering of primary cilia in confluent WT and *GANAB*^{-/-} cells detected for

acetylated α -tubulin (Ac. α -tub) and PC2, showing no cilia PC2 signal in *GANAB*^{-/-} cells. Scale bar = 10 μ m; DAPI stained nuclei; 100 ciliated cells analyzed (n=3) **(D)** Immunoblot of PC1 NT in WT and *GANAB*^{+/-} cells shows a reduced level of PC1-NTR in *GANAB*^{+/-} cells. Asterisk indicates a non-specific product¹⁶. **(E)** Quantification of PC1-NTR shows a reduction to ~50% ($p < 0.001$, Students T test) in heterozygous and complete loss in homozygous, *GANAB*^{-/-}, cells.

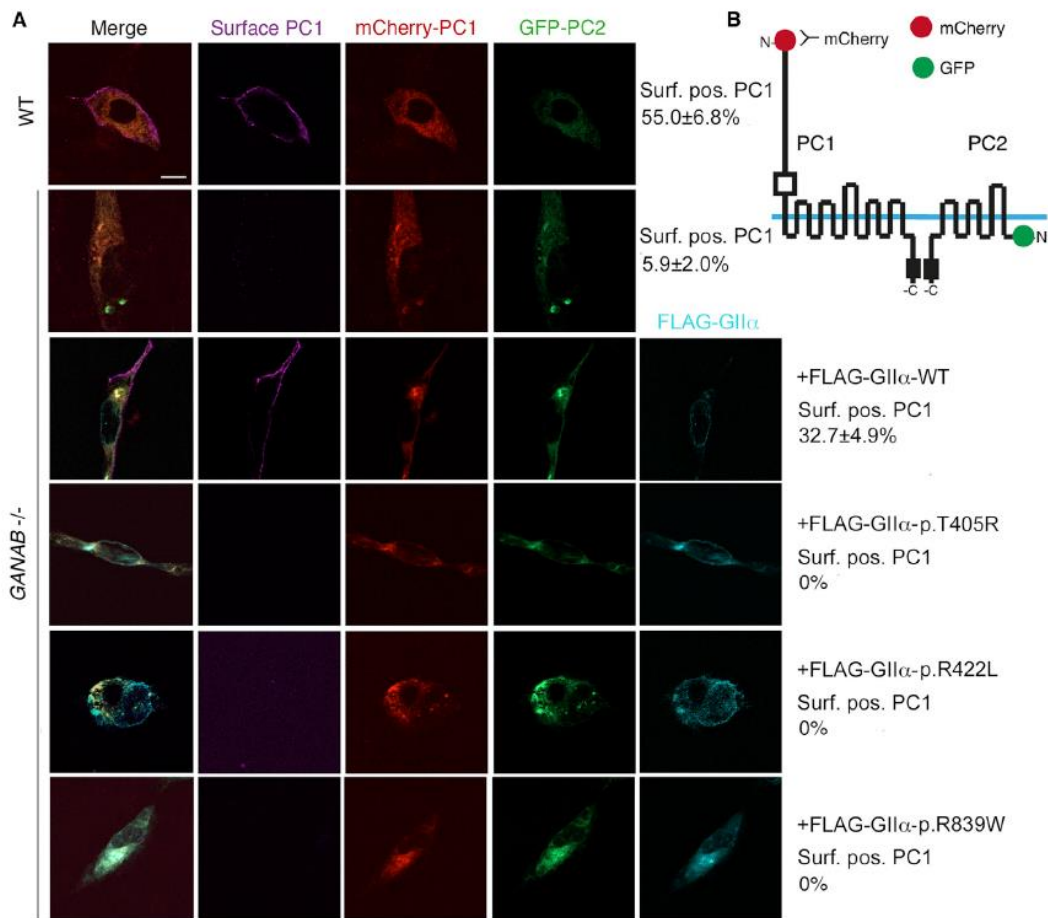


Figure 5: Surface localization of PC1 requires WT GII α and is disrupted by *GANAB* missense mutations.

(A) WT and *GANAB*^{-/-} cells co-transfected with WT tagged PC1 and PC2, mCherry-PC1 and TagGFP-PC2 (B), and examined for surface mCherry-PC1 labeling. Co-transfected cells were screened for live-cell surface PC1 signal and quantified as the percentage of surface positive PC1 relative to total co-transfected cells. Surface PC1 was detected on 55.0±6.8% of WT, but only 5.9±2.0% of *GANAB*^{-/-} cells ($P < 0.0001$), with the level rescued to 32.7±4.9% by co-transfection with the WT *GANAB* (FLAG-GII α) plasmid. Co-transfection with the newly identified putative *GANAB* missense mutations cloned in FLAG-GII α , p.Thr405Arg (p.T405R), p.Arg422Leu (p.R422L) and p.Arg839Trp (p.R839W), did not rescue PC1 surface localization (bottom three panels) (all $P < 0.0001$ vs. WT rescue). Student's T-test was performed to determine significance in at least 100 triple-transfected cells analyzed between three independent experiments. Scale bar=20 μ m.

Table 1. Clinical presentation of Autosomal Dominant Polycystic Kidney and Liver Disease in the 20 affected individuals from 9 *GANAB* mutant pedigrees

Pedigree	GANAB Mutation	Subject	Sex	eGFR ^b , age (y)	HBP ^c , age (y)	Type ^d	Age ^e	Radiologic Presentation					
								Kidneys			Liver		
								Cysts	Vol ^h	Fig.	Cysts	Vol ⁱ	Fig.
M263 ^a	c.1265G>T p.Arg422Leu	I-1	M	78, 66	N, 67	CT	66	~10 bilateral, largest 11 cm	302 ^k	1f	>50 scattered, largest 6 cm	1226	1f
		II-1	F	91, 42	N, 43	MRI	41	~10 bilateral, largest 3 cm	211	1g	>20 scattered, largest 3 cm	835	1g
M641	c.1914_1915delAG p.Asp640Glnfs*77	II-1	F	86, 51	Y, 40	CT	55	~15 bilateral, largest 10 cm	822 ^k	S3a	No liver cysts detected	1505 ^l	S3a
		II-2	F	104, 46	N, 50	CT	45	~10 bilateral, largest 6 cm	318 ^k	2b	~20 scattered, largest 2 cm	764	2b
290100	c.1914_1915delAG p.Asp640Glnfs*77	I-1	M	78, 65	N, 65	MRI	58	~8 bilateral, largest 2 cm	227	2e	>30 scattered, largest 3 cm	1255	2e
		II-1	M	87, 25	Y, 13	MRI	24	~12 bilateral, largest 2.5 cm	259	2d	None	832	2d
P1174	c.1214C>G p.Thr405Arg	I-1	M	N/A ^f	N, 61	US	55	3 cysts in the left kidney	NE	S3b	1 cyst, 1.5cm	NE	
		II-1	F	N/A ^f	N, 35	US	29	2 cysts in the right kidney	NE	2h	N/A	N/A	
		III-1	M	122, 9	N, 9	MRI	9	~5 bilateral, largest 2 cm	116	2g	None	492	
M656	c.2690+2_+7del	I-1	M	N/A ^f	Y, 55	CT*	67	Multiple small	NE	S3c	None	NE	S3c
		II-1	M	84, 39	N, 39	US	44	Multiple reported	N/A		Multiple reported	N/A	
		II-2	F	77, 50	N, 50	US	52	~5-10 bilateral, largest 2 cm	NE	S3d	>20 scattered, largest 5 cm	NE	S3d
		II-3	M	95, 49	Y, 35	MRI	43	>30 bilateral, largest 3 cm	SE	2l	>20 scattered, largest 1 cm	NE	2l
PK20016	c.39-1G>C	II-1	M	90, 53	Y, 45	CT*	52	~20 bilateral, largest 10 cm	665 ^k	3b	~20 scattered, largest 2 cm	1449 ^l	3b
PK20017	c.2176C>T p.Arg726*	II-1	F	77, 78	Y, 53	US	78	~40 bilateral, largest 3 cm	NE	3d	~20 scattered, largest 1.5 cm	N/A	3d
P1073	c.2515C>T p.Arg839Trp	I-2	F	N/A	N/A	US	(78)	Unknown	N/A		Multiple reported	N/A	
		II-1	F	86, 50	N	CT*	43	~8 bilateral, largest 1 cm	196	3f	Severe PLD, Tx 43y	4641 ^l	3f
		II-2	M	N/A	N/A	US	(44)	Unknown	N/A		Multiple reported	N/A	
M472	c.152_153delGA p.Arg51Lysfs*21	II-1	F	82, 58	N, 58	MRI	58	~20, largest 1 cm	223	3i	Severe PLD, resections 47y, 48y	1749 ^{jl}	3i
		II-2 ^g	F	N/A	N, 50	MRI	50	~16 bilateral, largest 6 cm	305 ^k	S3e	>50 scattered, largest 5 cm	1249 ^l	S3e

a. Mutation in this pedigree was first identified by whole exome sequencing. **b.** Based on last data available, expressed in ml/min/1.73m², obtained using the CKD-EPI formula in adults⁵⁰ and the Schwarz formula in the pediatric case⁵¹. **c.** High blood pressure (HBP), yes (Y) or no (N) and age at HBP diagnosis or BP measurement. **d.** CT=computerized tomography (CT) scan, CT*=contrast-enhanced CT scan, MRI=magnetic resonance imaging, US=ultrasound examination. **e.** Age at imaging examination. Values in parenthesis are present age if images not available. **f.** Kidney function was reported to be 'within the normal range'. **g.** Sample unavailable and so *GANAB* mutation not confirmed. **h.** Kidney volume measurement or estimate (Vol). Values are measured height adjusted total kidney volume (htTKV) ml/m; **k,** enlarged values, mean + 2SD of normal male and female htTKV⁴⁹; not (NE) or slightly enlarged (SE), estimated when full images not available; images not available (N/A). **i.** Liver volume measurement or estimate (Vol). Values are measured height adjusted total liver volume (htTLV) ml/m; **l,** enlarged values, mean + 2SD of normal male and female htTLV²⁷; not enlarged (NE), estimates when full images not available; images not available (N/A). **j**=htTLV after resections